(12)



SACLANTCEN MEMORANDUM
serial no.: SM-199

SACLANT ASW
RESEARCH CENTRE
MEMORANDUM



# The application of coupled-mode theory to propagation in shallow water with randomly varying sound speed

Rolf Thiele

June 1987



The SACLANT ASW Research Centre provides the Supreme Allied Commander, Atlantic (SACLANT) with scientific and technical assistance under the terms of its NATO charter, which entered into force on 1 February 1963. Without prejudice to this main task—and under the policy direction of SACLANT—the Centre also renders scientific and technical assistance to the individual NATO nations.

This document is released to a NATO Government at the direction of SACLANT ASW Research Centre subject to the following conditions:

- The recipient NATO Government agrees to use its best endeavours to ensure that the information herein disclosed, whether or not it bears a security classification, is not dealt with in any manner (a) contrary to the intent of the provisions of the Charter of the Centre, or (b) prejudicial to the rights of the owner thereof to obtain patent, copyright, or other like statutory protection therefor.

- If the technical information was originally released to the Centre by a NATO Government subject to restrictions clearly marked on this document the recipient NATO Government agrees to use its best endeavours to abide by the terms of the restrictions so imposed by the releasing Government.

Page count for SM-199
(excluding covers)

| Pages | Total |
|---|---|
| i–iv | 4 |
| 1–12 | 12 |
| @1–@17 | 17 |
| | 33 |

SACLANT ASW Research Centre
Viale San Bartolomeo 400
19026 San Bartolomeo (SP), Italy

tel: 0187 540 111
telex: 271148 SACENT I

NORTH ATLANTIC TREATY ORGANIZATION

SACLANTCEN SM-199

# The application of coupled-mode theory to propagation in shallow water with randomly varying sound speed

Rolf Thiele

---

The content of this document pertains to work performed under Project 19 of the SACLANTCEN Programme of Work. The document has been approved for release by The Director, SACLANTCEN.

Issued by:
Underwater Research Division

R. Thiele
Division Chief

intentionally blank page

# The application of coupled-mode theory to propagation in shallow water with randomly varying sound speed

Rolf Thiele

**Abstract:** Sound propagation in the Baltic Sea cannot be described correctly by range independent propagation models, even for areas with more or less constant water depths. The reason is the inability of such models to take account of the effect of forward scattering of sound produced by horizontal variations in the speed of the sound. Schneider and Sellschopp have simulated the forward-scattering effect by applying a parabolic equation method in conjunction with a Monte Carlo ray tracing program (MOCASSIN). This paper treats forward scattering in the normal mode concept, using the mode coupling formulation given by S.T. McDaniel. The mode coupling was added to the SUPERSNAP normal-mode code. Comparisons are made with the Schneider–Sellschopp calculations and with real data.

**Keywords:** Baltic, coupled-mode theory, MOCASSIN, mode coupling modelling, Monte Carlo ray tracing program, normal mode theory, propagation, scattering, shallow water, SNAP, sound speed, source localisation methods, transmission loss

## Contents



**Acknowledgement:** The measured acoustic data for case B of the numerical examples were provided by the Forschungsanstalt der Bundeswehr für Wasserschall und Geophysik, Kiel. My thanks also to M ∪. Ferla for introducing me to the SNAP model and to H. Schmidt for providing the plot programs.

## 1. Introduction

There are several basic methods which can be used to solve the wave equation for sound propagation in the ocean. However for shallow water it is the normal mode technique that is generally preferred [1]. This means solving the partial differential equation by separation of the variables in an orthogonal coordinate system, thereby converting to a set of ordinary differential equations. The boundary value equation in the vertical direction forms an eigenvalue problem. Each eigenfunction is an independent solution representing an individual wave propagating with a specific phase velocity and attenuation.

The basic theoretical assumption for the use of the normal mode technique is the horizontal invariance of the ocean. This rigorous requirement in the theory may be weakened to slow horizontal variations through the adiabatic approximation, which still neglects the transfer of energy from one mode to another (i.e. the mode coupling). Milder [2] and Pierce [3] reformulated the separation for slow horizontal variations with local eigenfunctions and included the effect of mode coupling.

McDaniel [4–6] used the Pierce formulation to calculate the coupling of modes by forward scattering. Her formulation was directed to horizontal variations of the sound speed. Nevertheless she reduced the application to horizontal variations of the boundaries.

Schneider [7,8] has shown that under certain conditions the forward scattering arising from variations in the sound speed may have a strong influence on the sound transmission loss. Therefore for the Baltic, where sound propagation is very sensitive to forward scattering, it is worthwhile using the McDaniel mode-coupling formulation.

The change of the transmission loss observed in the Baltic Sea is used to verify the mode coupling. However, even where the change of transmission loss is not significant, mode coupling may influence strongly the coherence of the sound field.

In principle the given method replaces the calculation of the sound field for range-dependent sound-speed profiles (which are not known deterministically) by a perturbation method that uses a range-independent modal computation for the mean sound-speed profile. The statistical expectation of the horizontal gradients of the sound speed profile is used for the calculation of the expected mode coupling.

## 2. Theory

The wave equation for harmonic time dependence is

$$\nabla^2\psi + k^2\psi = 0, \tag{1}$$

where $\psi$ is the wave velocity potential and the wave number $k = 2\pi f/c$ may vary arbitrarily with depth due to variation in the speed of sound $c$. The speed of sound is assumed to be slowly varying in the horizontal. We separate

$$\psi = \sum_{n=1}^{N} \Phi_n(x,y)u_n(z \mid x,y) \tag{2}$$

with $\Phi_n$ independent of $z$, where $u_n$ is a local eigenfunction of the $z$-separated part of the wave equation

$$\frac{\partial^2 u_n}{\partial z^2} + \left(k^2 - k_n^2\right) u_n = 0. \tag{3}$$

The function $u_n$ can be chosen such that the orthogonality relation

$$\int_0^H u_n(z)u_m(z)\,dz = \begin{cases} 1, & \text{for } n = m; \\ 0, & \text{otherwise} \end{cases} \tag{4}$$

is fulfilled. Then substituting Eq. (2) into Eq. (1), and multiplying by $\Phi_m$ and integrating over $z$ yields [2]:

$$\frac{\partial^2 \Phi_n}{\partial x^2} + \frac{\partial^2 \Phi_n}{\partial y^2} + k_n^2 \Phi_n = -\sum_{m \neq n} \left\{ A_{mn}\Phi_m + B_{mn}\frac{\partial \Phi_m}{\partial y} + C_{mn}\frac{\partial \Phi_m}{\partial x} \right\}, \tag{5}$$

where

$$A_{mn} = \int_0^H u_m \left( \frac{\partial^2 u_n}{\partial x^2} + \frac{\partial^2 u_n}{\partial y^2} \right) dz, \tag{6}$$

$$B_{mn} = 2\int_0^H u_m \frac{\partial u_n}{\partial y}\,dz, \tag{7}$$

$$C_{mn} = 2\int_0^H u_m \frac{\partial u_n}{\partial x}\,dz, \tag{8}$$

are coupling coefficients dependent on $x$ and $y$.

We propose for simplicity a propagation direction for $x$, such that $\partial\Phi/\partial y = 0$. Further, $\partial^2 u_n/\partial x^2$ is assumed small compared to $\partial^2\Phi_n/\partial x^2$. This means $A_{mn} = 0$ and $B_{mn} = 0$, reducing Eq. (5) to

$$\frac{\partial^2\Phi_n}{\partial x^2} + k_n^2\Phi_n = -\sum_{m\neq n} C_{mn}\frac{\partial\Phi_m}{\partial x}. \tag{9}$$

For computational reasons McDaniel [5] assumes a gaussian correlation function of the coupling coefficient

$$\langle C_{mn}(x+\Delta x)\cdot C_{mn}(x)\rangle \;=\; \langle C_{mn}^2\rangle e^{-\Delta x^2/L_x^2}, \tag{10}$$

where $L_x$ is the coupling correlation length. This assumption is discussed later.

The intensity of a single mode [1] is

$$p_n(x,z) \approx \left|\frac{\omega\rho}{4c}\sqrt{\frac{1}{2\pi x}}\frac{u_n(z_s)u_n(z)}{\sqrt{k_n}}e^{j(k_n+j\alpha_n)x}\right|^2. \tag{11}$$

The coupling may be described as the change in power of each mode, given by

$$\frac{\partial P_n}{\partial x} = \sum_{m=1}^{N} Q_{nm}P_m \tag{12}$$

with

$$P_n = \int_0^H p_n(x,z)\,dz.$$

Perturbation theory gives [4] for small coupling and $n \neq m$,

$$Q_{nm} = \frac{1}{4}\sqrt{\pi\frac{k_n}{k_m}}\langle C_{mn}^2\rangle L_x e^{-L_x^2/4(k_n-k_m)^2}. \tag{13}$$

Power conservation may be taken into account by

$$Q_{nn} = -\sum_{m\neq n} Q_{mn} - 2\alpha_n, \tag{14}$$

where $\alpha_n$ are the attenuation coefficients of the modes without coupling (i.e. volume attenuation in the water and in the bottom).

Furthermore, from McDaniel [5]:

$$C_{mn} = \frac{2}{k_n^2 - k_m^2}\int_0^H u_m\frac{\partial(k^2)}{\partial x}u_n\,dz. \tag{15}$$

To simplify the integral it is assumed $k_n \approx k_m \approx k$ and $c \approx c_0$, so that

$$C_{mn} = \frac{2k}{(k_m - k_n)c_0} \int_0^H u_m \frac{\partial c}{\partial x} u_n \, dz \tag{15a}$$

may be used.

The variance of the horizontal gradient of the sound-speed $\mathrm{grad}_x c = \partial c/\partial x$ is the basic oceanographic input for realistic calculations. This has to be depth dependent, as otherwise the orthogonality integral would yield

$$\int_0^H u_m \frac{\partial c}{\partial x} u_n \, dz = \frac{\partial c}{\partial x} \int_0^H u_m u_n \, dz = 0 \qquad \text{for } n \neq m,$$

with the result that coupling would be neglected.

In reality $\mathrm{grad}_x c$ should have a rather short correlation length in $z$. When this correlation length is small compared to the 'vertical wavelength' of the mode functions the double integral

$$\langle C_{mn}(x + \Delta x) C_{mn}(x) \rangle = \left[ \frac{2k}{(k_n - k_m)c_0} \right]^2$$

$$\times \int_0^H \int_{L_z} u_m(z) u_m(z + z') \left\langle \frac{\partial c(x + \Delta x, z)}{\partial x} \frac{\partial c(x, z + z')}{\partial x} \right\rangle u_n(z) u_n(z + z') \, dz' dz$$

may be reduced to

$$\langle C_{mn}^2 \rangle = \left[ \frac{2k}{(k_n - k_m)c_0} \right]^2 L_z \int_0^H u_m^2(z) u_n^2(z) \langle \mathrm{grad}_x^2 c(z) \rangle \, dz. \tag{16}$$

Eq. (16) can be applied directly to Eq. (13), giving the coefficients that are constant in $x$ for the linear system of differential equations of the first order Eq. (12).

This system of differential equations forms a standard real symmetric matrix eigenproblem

$$[Q - \lambda E] P = 0, \tag{17}$$

which is solvable by available library routines.

The resulting $N$ eigenvectors $P_n$, each with a constant $c_m$ and relative contribution coefficients $c_{mn}$ of the modes $m$ with $\sum_{m=1}^{N} c_{nm}^2 = 1$, form a set of independent solutions for the modes

$$P_n = \sum_{m=1}^{N} c_m c_{nm} e^{-\lambda_m x} \tag{18}$$

The coefficients $c_m$ are determined by inversion of the matrix of eigenfunctions, and using the initial values of the mode distribution

$$p_{m0} = \frac{\omega\rho}{4c}\frac{1}{2\pi k_m}\left|u_m(z_s)u_m(z)\right|^2 . \tag{19}$$

For large distances the eigenvector with the smallest attenuation will remain, giving the stationary solution with precisely this attenuation and range-independent vertical field distribution of the associated eigenfunction. The relation of the eigenvalues—which are attenuation coefficients—may be used to determine a range at which the cylindrical spreading law additionally to the mentioned attenuation will be applicable. Therefore this calculation will be a contribution to the everlasting discussion of whether shallow water propagation is best described by a $10\log r$ or a $15\log r$ range dependence.

## 3. The correlation function of the horizontal sound-speed gradient

The most comprehensive description of the variability of the internal structure of the ocean is the internal wave model of Garrett and Munk [9]. This model gives a spectral slope of $-2.5$.

Other authors [10,11] propose a wavenumber decay with an exponent of $-2$ (instead of $-2.5$) as more likely. Horizontal differentiation effects a multiplication of the horizontal wavenumber spectrum by the factor $k^2$, resulting in spectra for which the Fourier transforms are not performable by Riemann integrals [13].

This means that McDaniel's assumption of horizontal correlation in Eq. (10) is not justified, and consequently we cannot be sure whether the frequency dependence of the calculation is true.

Also, as this is a first approach there has to be a discussion of how to choose the horizontal correlation distance $L_x$, when we know that it may in reality be zero. The effect of $L_x$ on the coupling coefficients is twofold: it yields a scaling factor of the variance of the horizontal gradient and in the exponential part of Eq. (13) it yields a spatial low-pass filter for the modal interference. This second effect reduces the coupling of those modes with the larger differences of order; in other words it limits the angular spread of the associated rays. Since the coherence length should be shorter than the distance of modal interference (between a few meters and some 100 m) it is appropriate to eliminate this filtering effect.

The degeneration of a parameter with its horizontal coherence length may indicate a change in the power law of the associated process, i.e. a change in the wavenumber. Equation (13) exhibits a frequency-independent solution, which applies for large-scale scatterers [12]; for small-scale scatterers, a second-order dependence (Rayleigh scattering) is applicable.

Until now no actual measurements of the horizontal gradients were available for comparison. The assumed correlation lengths where justified by comparison of the mode conversion calculation using Baltic Sea propagation-loss experimental data with the parabolic-equation (PE) method of Schneider [8].

## 4. Coherence loss by mode conversion

Each mode has a certain phase velocity and all modes have a common initial phase. When the environment is known exactly, the interference pattern of the modes can be determined exactly, and conversely, with known modal structure the source position can be determined.

This deterministic phase relation is lost by the mode coupling process for two reasons:

- The difference in the phase velocities of the modes causes the phase of a converted mode to depend on the horizontal position of the conversion area.
- In the vertical direction the modes change in phase by 180° at each node, which means that the positions of the nodes of different modes are different and independent. Consequently, the resulting phase depends on the depth at which the coupling takes place.

One consequence of the mode conversion process is therefore a loss of phase information: the converted energy is incoherent, while the unconverted part of the sound field remains coherent.

The calculation of mode conversion can therefore yield an evaluation of coherence loss. This is valuable, because to estimate the coherence loss by directly measuring variations in the sound-speed profile is not easy.

## 5. Numerical examples

Two examples are given here of the use of the mode conversion (MC) process: case A gives the initial fit in comparison to Schneider and Sellschopp [8] and case B gives a typical example with a sound-speed profile that represents the Baltic duct. In both cases the real variations in the horizontal gradients were unknown.

Case *A*. Figures 1 to 4 show the rough range-depth distributions to be in good agreement. However the computations with and without horizontal variability show significant differences in the shapes of their contour lines. The reasons for these differences are:

- In the PE process the modes are added coherently and the interference has to be smoothed out by averaging in range and depth, whereas in the MC process the modes are added incoherently without averaging in range, and only in certain situations is there some averaging in depth.
- In the MC process the assumed stationary variations of the sound-speed profiles are used to derive a mean solution, whereas in the PE process an experimentally-determined, individual two-dimensional sound-speed profile is used.
- For these rather high frequencies Schneider was forced to run the PE process with the minimum acceptable resolution in order to save computer time. Thus, some numerical inaccuracies are to be expected.
- Possibly there is some error in the MC process as a consequence of the conversion to the continuous part of the modal spectrum being neglected.

In addition the computation without coupling and mode conversion shows significant differences in the absolute values of the transmission loss; these can not be explained at present. A calibration error in the PE calculation is a possible reason.

The type of depiction used is rather sensitive to errors, since the volume attenuation is neglected in both calculations. As a result the residual attenuation is low and errors are relatively enhanced.

What is remarkable is that the energy scattered into the duct is markedly frequency-independent, and is close to 100 dB at about 25 km. This is in accordance with Mellen et al. [14], who suggest that the loss attributable to forward scattering will be frequency independent. The energy in the duct is only attenuated by scattering and geometrical spreading, because volume attenuation is not introduced and no direct bottom interaction takes place.

Case *B*. This case deals with the comparison of the MC process with reality, whereas case A concerned a comparison with another computational method using

the same data.

Relative to case A, the assumed horizontal gradients had to be increased by a factor of 10 before good agreement was achieved. This is surprising, since the temperature profiles of case A were measured in a similar area of the Baltic as the acoustic measurements of case B.

Three explanations for this difference are offered:

(1) The absolute calibration error referred to above leads to a wrong fit. Increasing the average horizontal gradients in case A would increase the scattered energy by approximately 10 dB. This is still within the calibration difference of the PE process and the mode conversion process without coupling.

(2) The horizontal spacing of the measurements for the temperature profiles was about 100 m. In the PE process a linear interpolation is introduced between the measured profiles. To get correct results the spacing of the profiles has to be shorter than the horizontal correlation length of the temperature field or possibly of the horizontal gradients of it. Unfortunatly the correlation length of the horizontal gradients is expected to be shorter, and then the interpolation means a low-pass filtering of the original field which reduces the average horizontal gradients.

(3) Knowledge about the changes of the horizontal gradient field in complicated areas such as the Baltic is inadequate. In this environment gradients will be produced more by changes of the salinity and temperature of the water masses in a density balance than by internal waves. Therefore changes in the average gradients by a factor of 10 are not unlikely, since the measurements are not taken at the same position.

Figure 5 shows the comparison with the measured data. The shallow receivers exhibit the effect of the mode coupling significantly. The range-independent solution is completely wrong for this situation: with increasing frequency a difference in the stationary attenuation arises, presumably because the volume attenuation in the low salinity water was not taken correctly into account. In the model computation the attenuation is reduced proportional to the salinity according to the Thorpe attenuation [15], but the correct low salinity attenuation is still controversial [16]. The data show the parallelism of the transmission loss in the duct and beyond as being in agreement with the mode coupling. The spacing between these parallel curves is correct for all frequencies.

In case A it was shown that the amount of scattered energy is almost frequency dependent. But this is not the case for the change in the vertical structure of the transmission loss. In Fig. 6a at 250 Hz, there is nearly no influence by mode coupling at 10 km, and at 50 km only the difference outside the duct is significant. At 500 Hz (Fig. 6b) the fine structure in the duct is smoothed out at 10 km, while

the general tendency of the vertical transmission loss does not change even at 10 km. At 1 kHz (Fig. 6c) this change in the fine structure is observed at 3 km; at 10 km the structure changes significantly.

With increasing frequency the transmission loss profile is smoothed by the coupling, giving a range independent structure (Figs. 6d and e) which is a projection of the sound-speed profile (Fig. 13). This may be observed best at the small change in sound speed at 65 m and the strong vertical gradient at 90 m. Between the corner points of the sound-speed polygon which are depicted in the transmission loss profile, the transmission loss changes very smoothly.

The reason why the energy distribution in the scattering process seems to be almost independent of frequency while the vertical structure of the transmission loss is strongly dependent on frequency, becomes evident when one looks at the mode spectra. Figures 7 to 10 show the energy distribution of the modes, each with their ray angle corresponding to the minimum value of the sound speed.

In Figs. 7 to 10 the range of 1 m is only given as a reference of the mode distribution for the source. The values were extrapolated from the far field, as the far-field solution of the Hankel functions is also applied for this short range. The figures were obtained via the plotting program for the mode intensity versus angle of the SNAP program [1]. However, it is the complete mode energy in the given range that is depicted, and not the intensity of the modes at a single receiver depth.

Figure 7b (the uncoupled result) reveals some relation to the distribution of Fig. 7a. There are significant differences between the individual modes, and the high-order modes are strongly attenuated. The coupled modes have a rather smooth envelope.

Figure 8a shows the initial distribution with the source outside the duct. In Fig. 8b it is obvious that the peculiarities of the initial distribution are better retained by the uncoupled solution; however, some of the initial structure is visible in both the coupled and the uncoupled results.

Figures 9a and b show that the source depth has a much stronger influence at higher frequencies. For the uncoupled situation the source pattern is maintained for all modes up to mode 40, i.e. the propagation effects a 'low-pass mode-filtering' with a cut-off at approximately the 40th mode (Fig. 9c).

With the receiver outside the duct only the modes above the 100th are excited (Fig. 9b). Therefore only residual modes are left, and the mode spectrum is thinned out (Fig. 9d).

With mode coupling (Figs. 9e and f) we find a completely different situation. The envelope of the mode spectrum is rather smooth, with nothing left of the initial

pattern. The figures that have different source depths are only distinguishable by the different common levels of all modes.

Figures 10a to d show the results for different frequencies and source depths. The similarity of the envelopes is evident. The envelope reflects some of the relations between the sound-speed profiles and the attenuation in the bottom. Its main feature is similar for all frequencies but it is contorted with frequency.

The paradox of the level of scattered energy (case A) seeming to be frequency independent while the structural changes are strongly frequency dependent may now be answerable. The level of scattered energy is determined by the envelope of the mode spectrum. The envelope is only weakly frequency dependent for the coupled mode result but strongly so for the uncoupled result. The higher modes are heavily attenuated at high frequencies. Equation (16) reveals that the coupling between the modes is proportional to the squared reciprocal of the relative wave number difference corresponding to the absolute angular difference. Therefore the coupling is strong at high frequencies, with the angles close together, and the fine structure of the mode spectrum is smoother at higher frequencies.

Figure 11 shows examples of the transmisson loss over range and depth similar to those for Figs. 1 to 4 (case A). There is a remarkable similarity between Figs. 11d and e, which relates to different source depths. The sound speed profile is again duplicated in the contour lines.

The coherence of the sound field is demonstrated by Fig. 12. Although the vertical structure of the coherence depends on the source depth, the range of each individual contour line is on average independent of the source depth. However, the coherence can be said to depend strongly on the frequency, since the neighbouring modes interact strongly at high frequencies. This does not affect the transmission loss significantly, but the coherence is lost whenever there is mode conversion.

## 6. Conclusions

Forward scattering attributable to sound-speed variations strongly affects propagation in the Baltic. This was shown by Schneider and Sellschopp using the parabolic equation (PE) process [8] and is here demonstrated by a mode coupling (MC) method.

Variable sound-speed profiles have a strong effect on both the transmission loss and the coherence of propagation. The forward scattering can not only increase the attenuation but also—with the source or receiver beyond the optimum depth—reduce it.

This report only treats forward scattering caused by sound-speed variations. Essen and Hasselmann [17] treated the mode coupling by the sea-surface roughness and McDaniel [6] that by the bottom. Boundary scattering has to be incorporated in the computer code as a next step. Also, quantitative measurements on horizontal sound-speed gradients have to be made together with acoustic measurements.

The mode coupling method yields a redistribution of intensity in the vertical plane. This redistribution is only dependent on the sound-speed structure, not on the source depth. When energy is scattered into the duct from outside or vice versa, the ratio of the scattered energy to the total energy seems to be almost frequency-independent. The total amout of mode-converted energy, however, is strongly frequency-dependent.

The method of mode coupling that has been used is a powerful tool for the description of random forward scattering. It is not dependent on the mathematical simplifications of the ray theory, which prevent direct calculation of frequency-dependent effects. The calculation is relatively simple and fast and the coupling calculations are equivalent to about 10% of the mode calculations. In the same way as conventional mode calculations they provide solutions for arbitrary ranges without range dependence penalties.

Mode coupling always affects the coherence of the sound field, and so the technique described helps in defining limits for source localisation methods that make use of the modal structure.

## References


[1] JENSEN, F.B. and FERLA, M.C. SNAP: the SACLANTCEN normal-mode propagation model, SACLANTCEN SM-121. La Spezia, Italy, SACLANT ASW Research Centre, 1979. [AD A 067 256]

[2] PIERCE, A.D. Extension of the method of normal modes to sound propagation in an almost-stratified medium. *Journal of the Acoustical Society of America* **37**, 1965: 19–27.

[3] MILDER, D.M. Ray and wave theory invariants for SOFAR channel propagation. *Journal of the Acoustical Society of America* **46**, 1969: 1259–1263.

[4] McDANIEL, S.T. Coupled power equation for cylindrically spreading waves. *Journal of the Acoustical Society of America* **60**, 1976: 1285–1289.

[5] McDANIEL, S.T. Mode conversion in shallow-water sound propagation. *Journal of the Acoustical Society of America* **62**, 1977: 320–325.

[6] McDANIEL, S.T. Calculation of mode conversion rates. *Journal of the Acoustical Society of America* **63**, 1978: 1372–1374.

[7] SCHNEIDER, H.G. Excess sound propagation loss in a stochastic environment. *Journal of the Acoustical Society of America* **62**, 1977: 871–877.

[8] SCHNEIDER, H.G. and SELLSCHOPP, J. Transmission loss computations from sound speed data of high horizontal resoution with strong variability. FWG-Report 1981-12. Kiel, Forschungsanstalt der Bundesweht für Wasserschall und Geophysik, 1981.

[9] GARRETT, C. and MUNK, W. Space-time scales of internal waves: a progress report. *Journal of Geophysical Research* **80**, 1975: 291–297.

[10] EWART, T.E. Acoustic fluctuations in the open ocean—a measurement using a fixed refracted path. *Journal of the Acoustical Society of America* **67**, 1980: 496–503.

[11] DESAUBIES, Y.J.F. Analytical representation of internal wave spectra. *Journal of Physical Oceanography* **6**, 1976: 1976–1981.

[12] CHERNOV, L.A. Wave Propagation in a Random Medium. New York, N.Y., McGraw-Hill, 1960.

[13] PAPOULIS, A. The Fourier Integral and its Applications. New York, N.Y., McGraw-Hill, 1962: pp. 251–252.

[14] MELLEN, H.G., BROWNING, D.G. and ROSS, D.J.R. Attenuation in randomly inhomogeneous sound channels. *Journal of the Acoustical Society of America* **56**, 1974: 80–82.

[15] THORPE, W.H. Analytic description of the low-frequency attenuation coefficient. *Journal of the Acoustical Socey of America* **42**, 1967: 270–271.

[16] SCHNEIDER, H.G., THIELE, R. and WILLE, P.C. Measurement of sound absorption in low salinity water of the Baltic Sea. *Journal of the Acoustical Society of America* **77**, 1985: 1409–1412.

[17] ESSEN, H.H. and HASSELMANN, H. Scattering of low-frequency sound in the ocean. *Zeitschrift für Geophysik* **36**, 1970: 655–678.

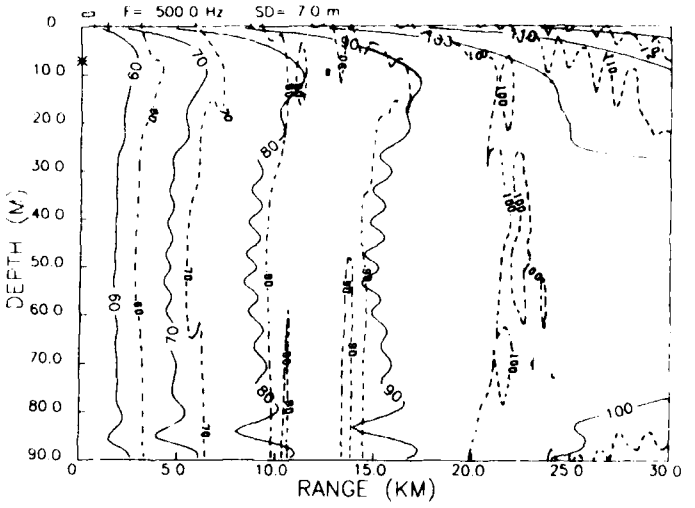


*Fig. 1. Case A: comparison of forward scattering by coupled modes (solid lines) with parabolic equation [7] (dashed lines); transmission loss over range and depth for a 7 m deep source at 500 Hz.*

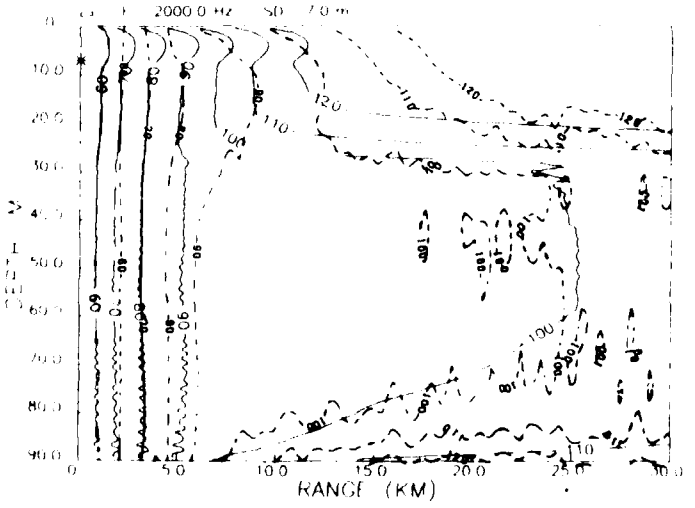


*Fig. 2. Case A: comparison of forward scattering by coupled modes (solid lines) with parabolic equation [7] (dashed lines), transmission loss over range and depth for a 7 m deep source at 2000 Hz*

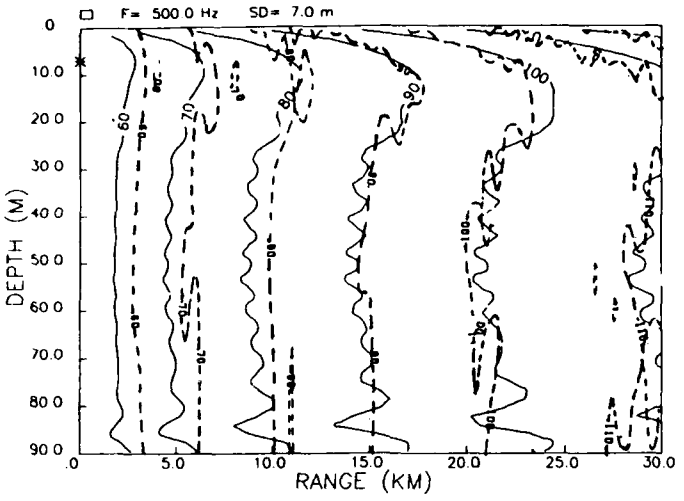


*Fig. 3. Case A: comparison of forward scattering without mode coupling (solid lines) and parabolic-equation calculation (dashed lines) for a single sound-speed profile; transmission loss over range and depth for a 7 m deep source at 500 Hz.*

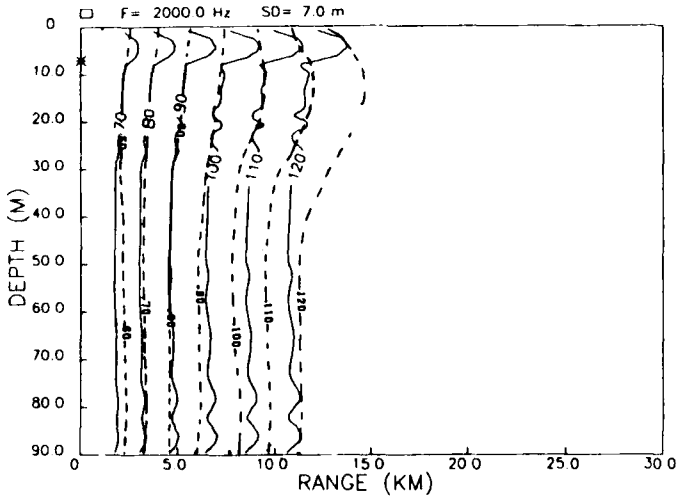


*Fig. 4. Case A: comparison of forward scattering without mode coupling and parabolic-equation calculation for a single sound-speed profile; transmission loss over range and depth for a 7 m deep source at 2000 Hz.*

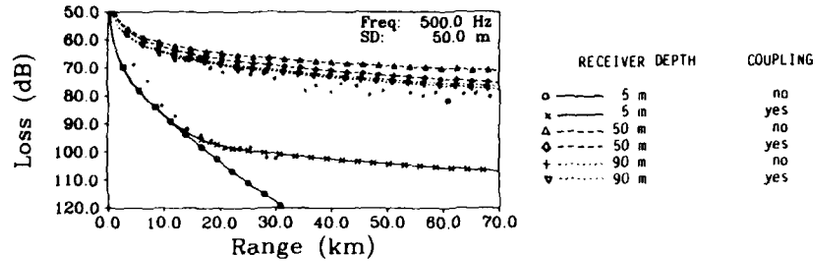


*Fig. 5a. Case B: transmission loss at 500 Hz; calculated (lines) and measured (dots).*

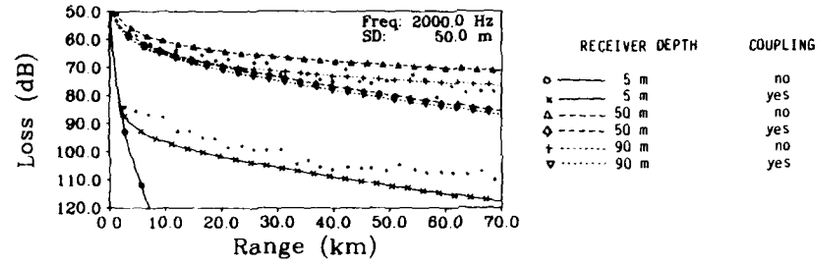


*Fig. 5b. Case B: transmission loss at 2 kHz; calculated (lines) and measured (dots).*

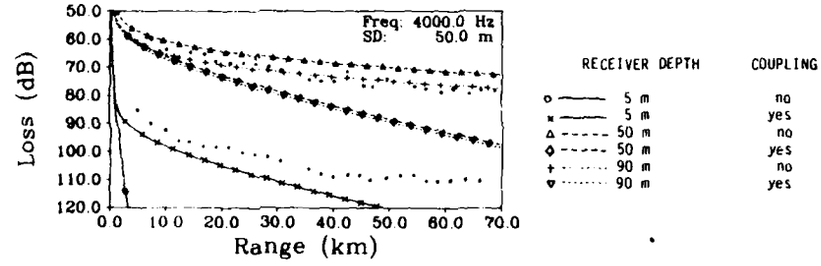


*Fig. 5c. Case B: transmission loss at 4 kHz; calculated (lines) and measured (dots).*

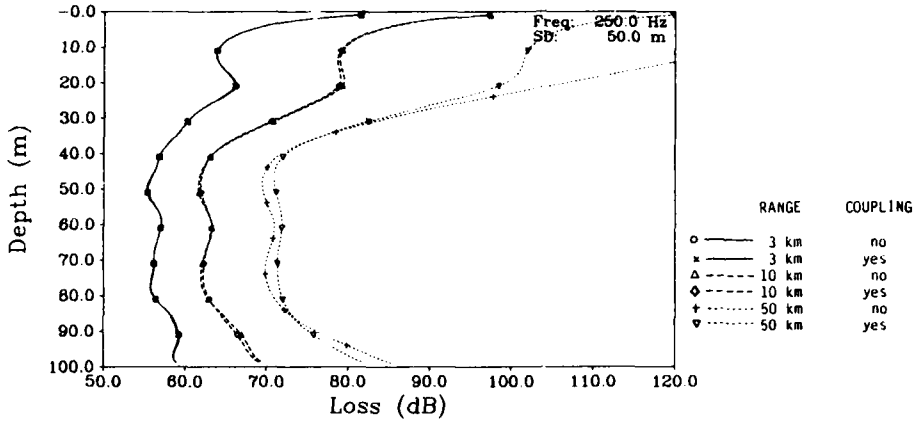


*Fig. 6a. Case B: transmission loss as a function of depth with range with and without coupling as parameter; frequency 250 Hz.*

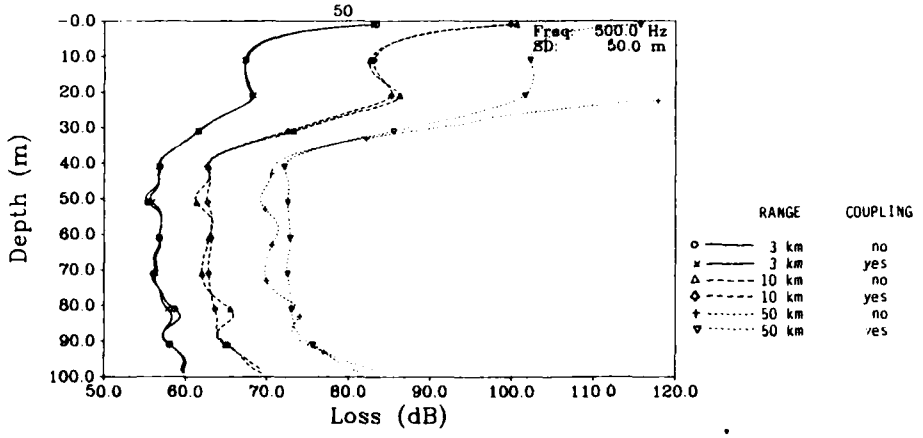


*Fig. 6b. Case B: transmission loss as a function of depth with range with and without coupling as parameter; frequency 500 Hz.*

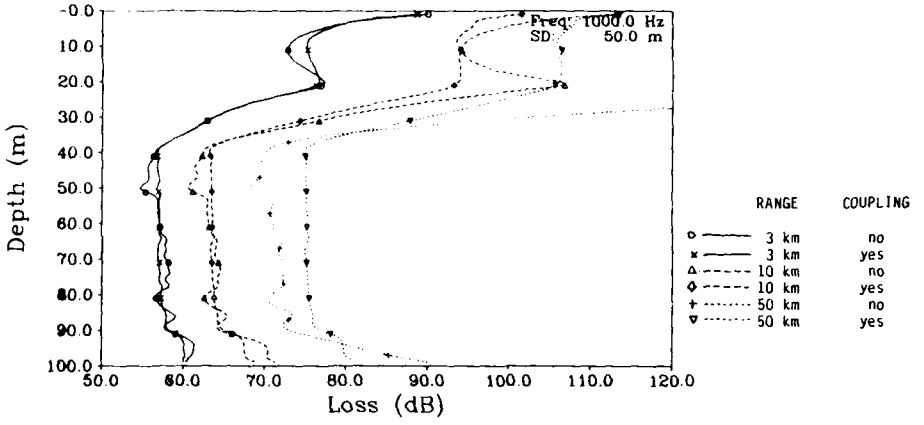


*Fig. 6c. Case B: transmission loss as a function of depth with range with and without coupling as parameter, frequency 1 kHz.*

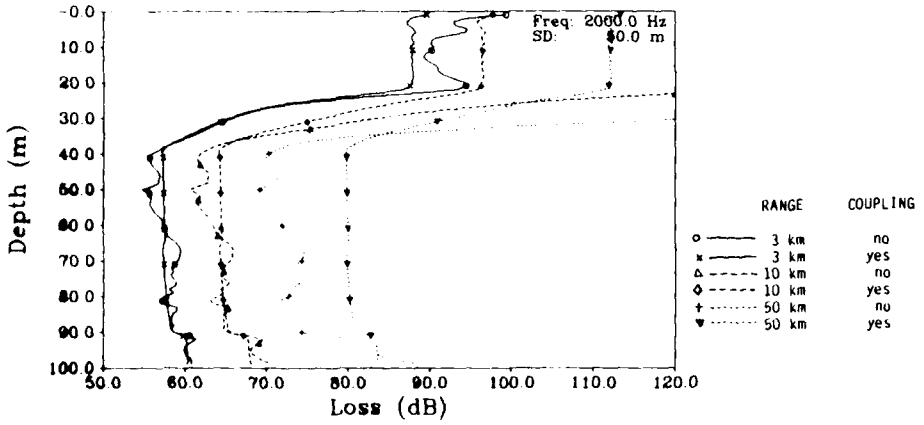


*Fig. 6d. Case B: transmission loss as a function of depth with range with and without coupling as parameter, frequency 2 kHz.*

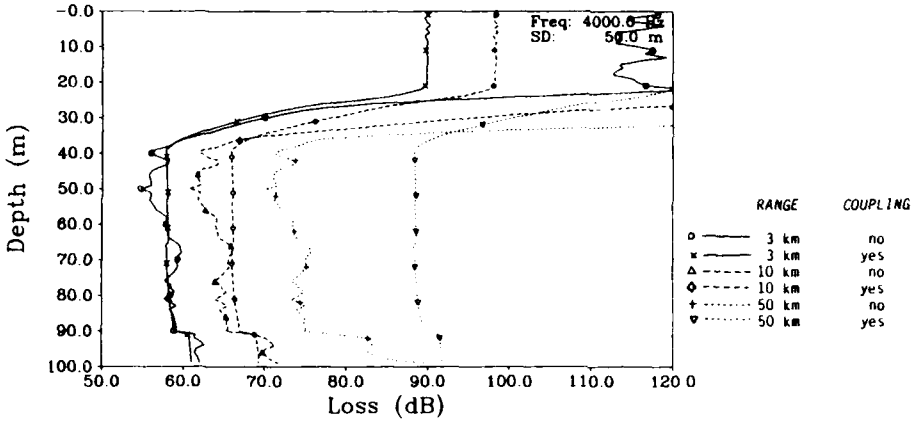


*Fig. 6e. Case B: transmission loss as a function of depth with range with and without coupling as parameter, frequency 4 kHz.*

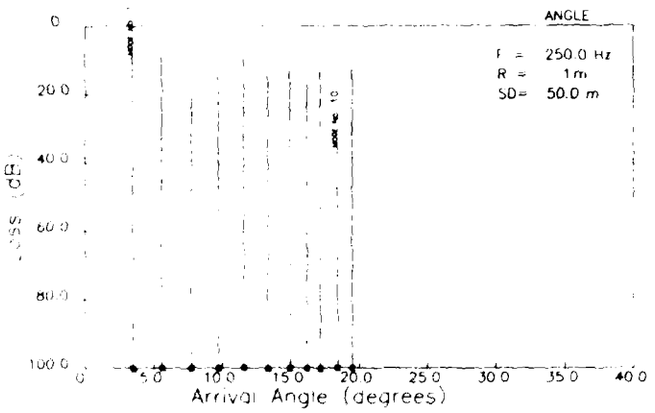


*Fig. 7a Distribution of modes by excitation in 50 m depths at 250 Hz*

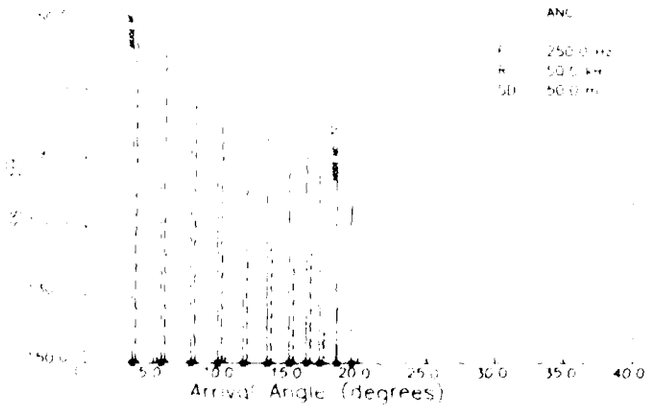


***Fig. 7b Mode distribution after 50 km propagation, solid lines with coupling, dashed lines without coupling***

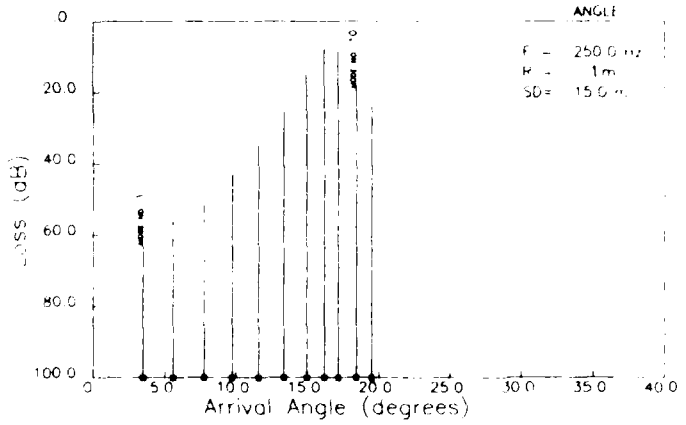


*Fig. 8a. Mode excitation at range 1 m for a source at 15 m depth, frequency 250 Hz*

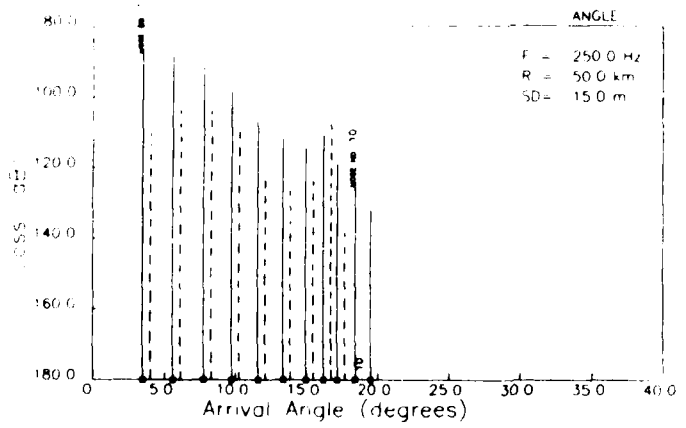


***Fig. 8b. Mode distribution for 15 m source after 50 km propagation, solid lines: with mode coupling, dashed lines: without coupling.***

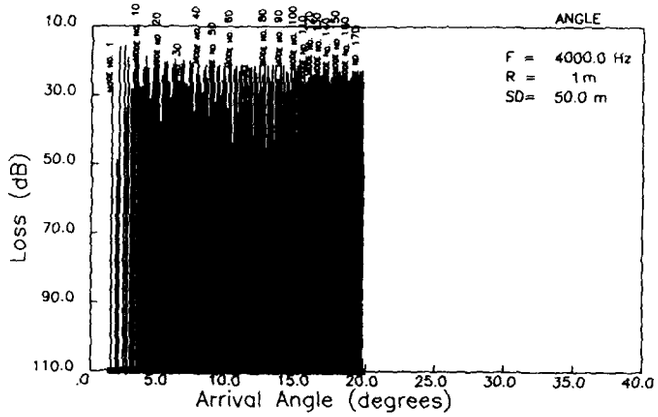


*Fig. 9a. Mode excitation at 4 kHz for 50 m source.*

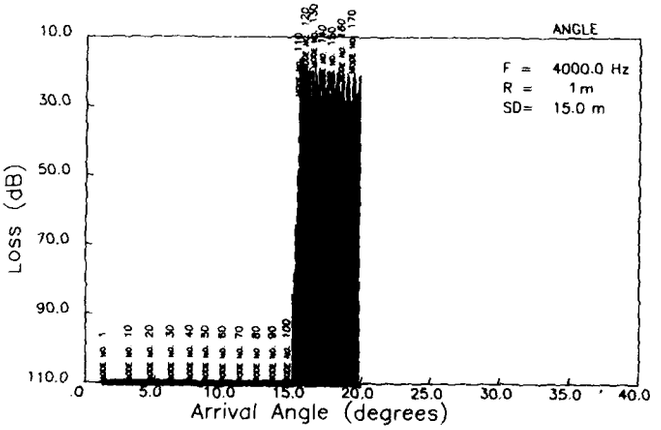


*Fig. 9b. Mode excitation at 4 kHz for shallow source.*

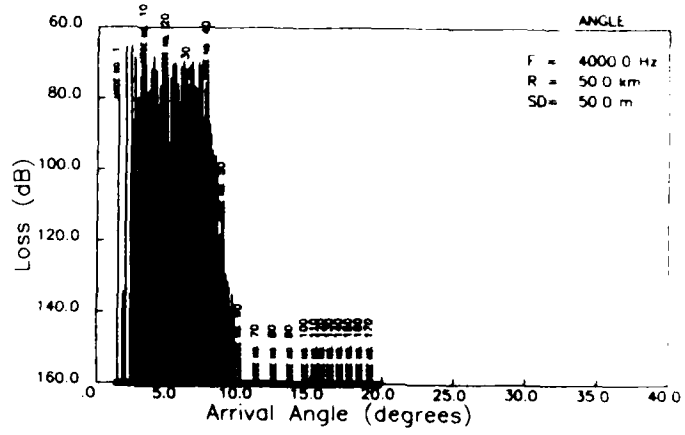


*Fig. 9c. Mode excitation at 4 kHz and deep source after 50 km propagation, without coupling*

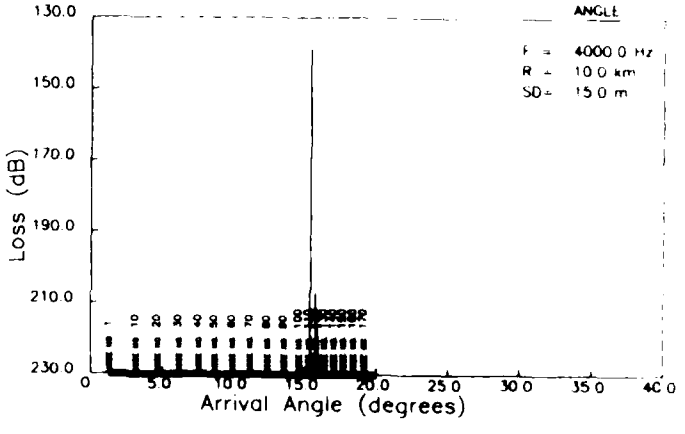


*Fig. 9d. Mode excitation at 4 kHz for shallow source after 10 km propagation, without coupling*

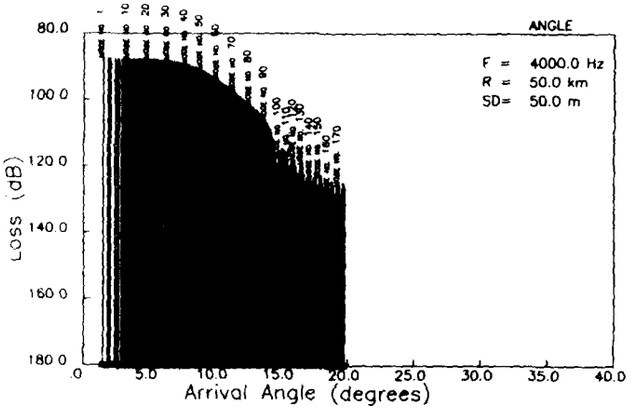


*Fig. 9e. Mode excitation at 4 kHz for deep source after 50 km propagation, with coupling.*

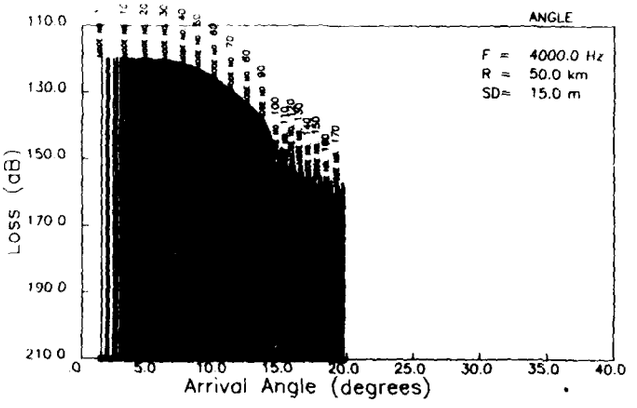


*Fig. 9f. Mode excitation at 4 kHz for shallow source after 50 km propagation, with coupling.*

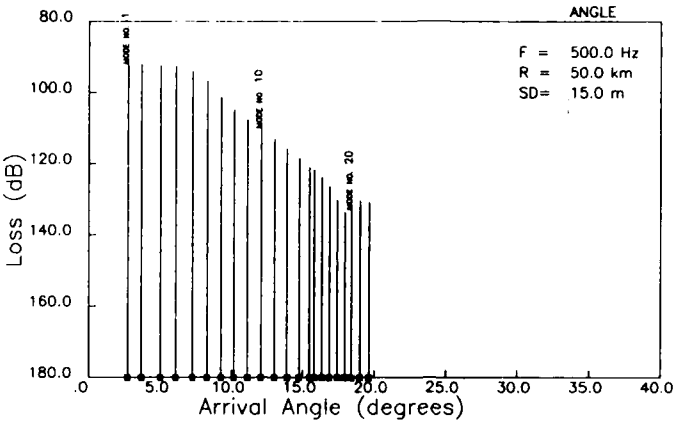


*Fig. 10a. Mode spectrum at 500 Hs after 50 km propagation, with coupling, source depth 15 m.*

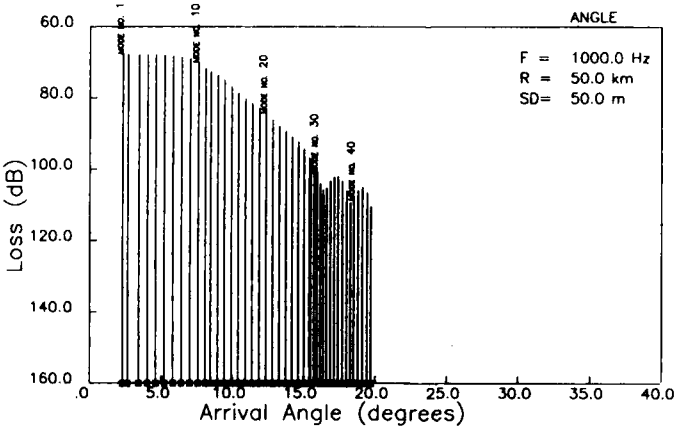


*Fig. 10b. Mode spectrum at 1 kHs after 50 km propagation, with coupling, source depth 50 m.*

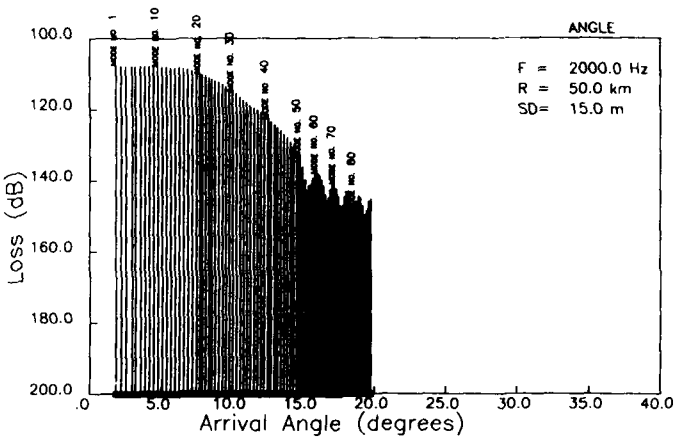


*Fig. 10c. Mode spectrum at 2 kHz after 50 km propagation, with coupling, source depth 15 m.*

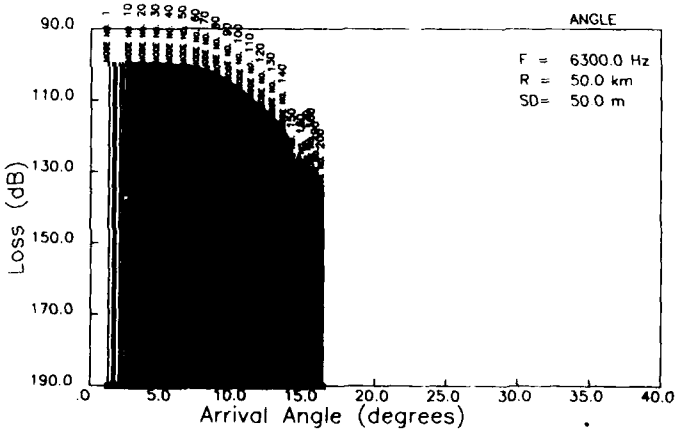


***Fig. 10d. Mode spectrum at 6.3 kHz after 50 km propagation, with coupling, source depth 50 m. With respect to the computation time and the dimension of the data fields only the lowest 200 modes were calculated.***

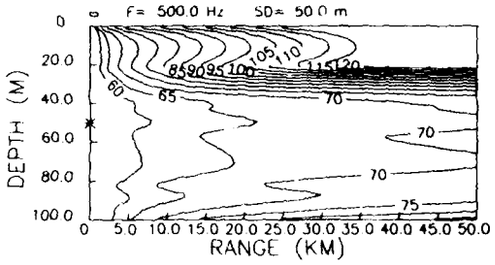


*Fig. 11a. Case B: transmission loss over range and depth at 500 Hz, without mode coupling.*

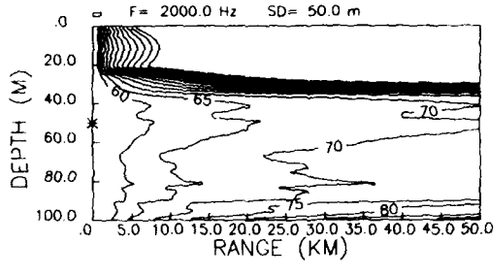


*Fig. 11b. Case B: transmission loss over range and depth at 2 kHz, without mode coupling.*

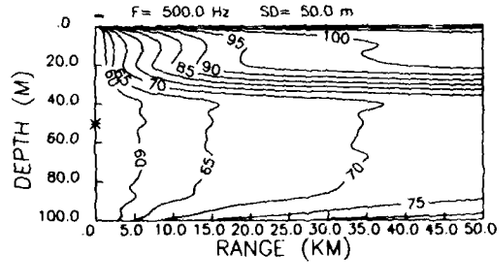


*Fig. 11c. Case B: transmission loss over range and depth at 500 Hz, with mode coupling.*

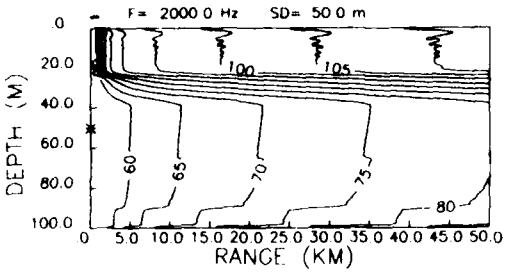


*Fig. 11d. Case B: transmission loss over range and depth at 2 kHz, with mode coupling.*

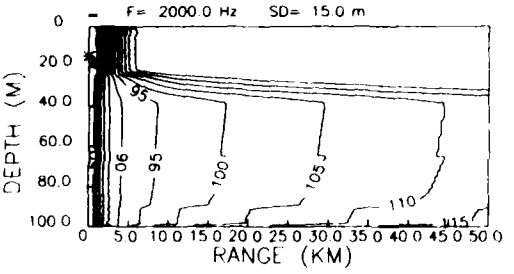


*Fig. 11e. Case B: transmission loss over range and depth at 2 kHz, with mode coupling, source beyond the duct. The steps in the 105 dB line are an artefact produced by the limited resolution of levels of 0.1 dB provided to the contour program.*

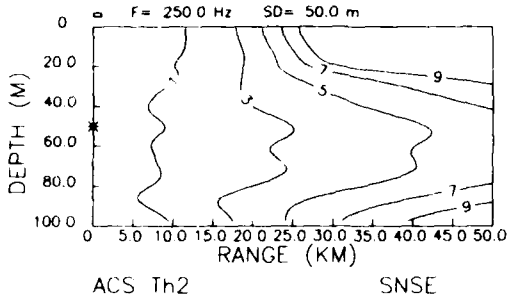


*Fig. 12a. Relative content of coherent sound intensity (in dB) as a function of range and depth; frequency 250 Hz, source depth 50 m.*

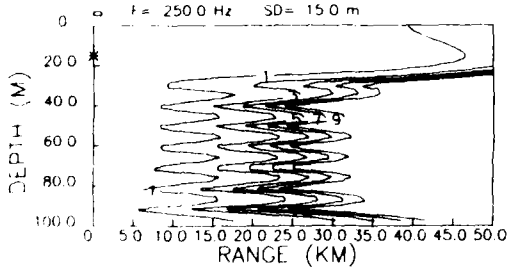


*Fig. 12b. Relative content of coherent sound intensity (in dB) as a function of range and depth; frequency 250 Hz, source depth 15 m.*

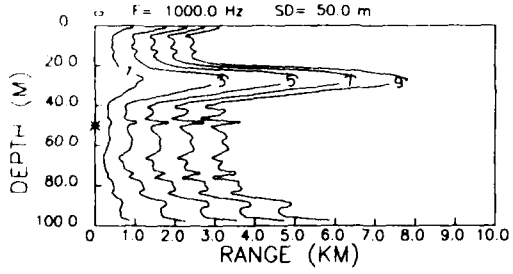


*Fig. 12c. Relative content of coherent sound intensity (in dB) as a function of range and depth; frequency 1 kHz, source depth 50 m.*

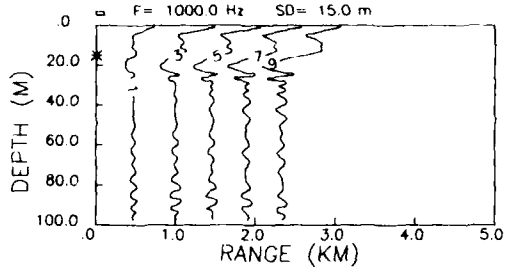


*Fig. 12d. Relative content of coherent sound intensity (in dB) as a function of range and depth; frequency 1 kHz, source depth 15 m.*

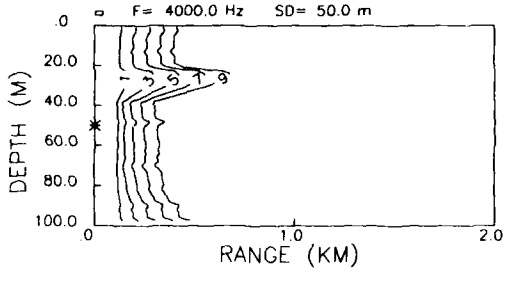


*Fig. 12e. Relative content of coherent sound intensity (in dB) as a function of range and depth; frequency 4 kHz, source depth 50 m.*

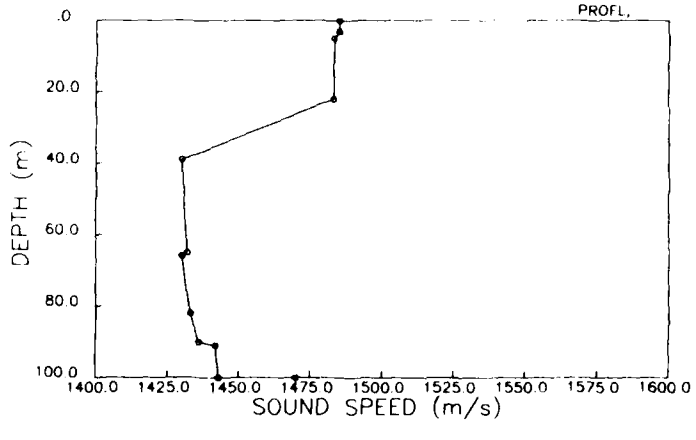


***Fig. 13. Case B: sound speed profile.***

## Initial Distribution for SM-199

| | |
|---|---|
| *Ministries of Defence* | |
| JSPHQ Belgium | 2 |
| DND Canada | 10 |
| CHOD Denmark | 8 |
| MOD France | 8 |
| MOD Germany | 15 |
| MOD Greece | 11 |
| MOD Italy | 10 |
| MOD Netherlands | 12 |
| CHOD Norway | 10 |
| MOD Portugal | 2 |
| MOD Spain | 2 |
| MOD Turkey | 5 |
| MOD UK | 20 |
| SECDEF US | 68 |
| *NATO Authorities* | |
| Defence Planning Committee | 3 |
| NAMILCOM | 2 |
| SACLANT | 10 |
| SACLANTREPEUR | 1 |
| CINCWESTLANT/ COMOCEANLANT | 1 |
| COMSTRIKFLTANT | 1 |
| COMIBERLANT | 1 |
| CINCEASTLANT | 1 |
| COMSUBACLANT | 1 |
| COMMAIREASTLANT | 1 |
| SACEUR | 2 |
| CINCNORTH | 1 |
| CINCSOUTH | 1 |
| COMNAVSOUTH | 1 |
| COMSTRIKFORSOUTH | 1 |
| COMEDCENT | 1 |
| COMMARAIRMED | 1 |
| CINCHAN | 3 |
| *SCNR for SACLANTCEN* | |
| SCNR Belgium | 1 |
| SCNR Canada | 1 |
| SCNR Denmark | 1 |
| SCNR Germany | 1 |
| SCNR Greece | 1 |
| SCNR Italy | 1 |
| SCNR Netherlands | 1 |
| SCNR Norway | 1 |
| SCNR Portugal | 1 |
| SCNR Turkey | 1 |
| SCNR UK | 1 |
| SCNR US | 2 |
| SECGEN Rep. SCNR | 1 |
| NAMILCOM Rep. SCNR | 1 |
| *National Liaison Officers* | |
| NLO Canada | 1 |
| NLO Denmark | 1 |
| NLO Germany | 1 |
| NLO Italy | 1 |
| NLO UK | 1 |
| NLO US | 1 |
| *NLR to SACLANT* | |
| NLR Belgium | 1 |
| NLR Canada | 1 |
| NLR Denmark | 1 |
| NLR Germany | 1 |
| NLR Greece | 1 |
| NLR Italy | 1 |
| NLR Netherlands | 1 |
| NLR Norway | 1 |
| NLR Portugal | 1 |
| NLR Turkey | 1 |
| NLR UK | 1 |
| Total external distribution | 248 |
| SACLANTCEN Library | 10 |
| Stock | 22 |
| Total number of copies | 280 |

END